Final Draft

of the original manuscript

Xu, Y.; Gavras, S.; Gensch, F.; Kainer, K.; Hort, N.:

Effect of Nd Additions on the Mechanical Properties of Mg Binary Alloys.

In: JOM: The Journal of the Minerals, Metals and Materials Society. Vol. 72 (2020) 1, 517 - 522.

First published online by Springer: 25.10.2019

https://dx.doi.org/10.1007/s11837-019-03877-y

Effect of Nd Additions on the Mechanical Properties of Mg Binary Alloys

Yuling Xu[1,*], Sarkis Gavras[2], Felix Gensch[3], Karl Ulrich Kainer[2], Norbert Hort[2,*]

[1]Shanghai Spaceflight Precision Machinery Institute, Shanghai 201600, China

[2]MagIC-Magnesium Innovation Center, Helmholtz-Zentrum Geesthacht, 21502 Geesthacht, Germany

[3]TU Berlin, Forschungszentrum Strangpressen, Gustav-Meyer-Allee 25, 13355 Berlin, Germany

Abstract

The influence of Nd contents and particles on the microstructure and mechanical properties of extruded Mg alloys are discussed. Pure Mg and binary Mg–xNd (x = 0.2, 0.5, 1, 2, 5 wt.%) alloys were cast and extruded. Hardness and tensile/compression tests were measured on those alloys. The results show that the addition of Nd to Mg leads to improvements in hardness, tensile/compression yield strengths and elongation. However, the Nd has little effect on ultimate strengths and compressibility of Mg alloys. The contributions of strengthening mechanisms to the tensile/compressive yield strength of extruded Mg–Nd alloys are investigated. $Mg_{41}Nd_5$ phase was distributed in Mg–2Nd and Mg–5Nd alloys after extrusion which is the main reason that decreased the grain size of Mg–Nd. The tension-compressing yield asymmetry is decreased from 1.8 to 1 with the increased additions Nd in extruded alloys.

Key words:

Mg–Nd alloy, Particles, Hardness, Yield strength.

1 Introduction

In the past few decades, a large amount of studies has been focused on designing and developing the light structure materials. Magnesium and its alloys as one of lightest weight structure materials, have good casting and recycling properties with low cost and are used in special application fields, such as aerospace, engineering and automobile industries [1, 2]. Compare with casting alloys, Mg alloys after extrusion exhibit much higher mechanical properties of Mg alloys, such as yield stress, ultimate stress and ductility. However, the extruded Mg alloys also have drawbacks, which are that the strong texture and asymmetry of mechanical properties. Many previous researches show that the mechanical properties of Mg alloys have been significantly improved by adding

REs (rare earth elements) [3-5]. Furthermore, extruded Mg alloys with more random textures can be developed with Res [6, 7].

Both solid solutes andparticles have strengthening effects on the mechanical properties of Mg alloys [6, 8, 9]. The specific selections of alloying elements and/or processing steps such as heat treatment allow for the proper processing and the formation of a microstructure that can be useful for the selected purpose [10, 11].

In comparison to some other RE elements, Nd has relatively low maximum solid solubility in Mg (0.63 at.% Nd at the eutectic temperature) [12]. Many researchers reported that alloying with Nd has an efficient effect on improving the mechanical properties of Mg alloys [13, 14]. In order to investigate the mechanical strengthening mechanism and the yield stress asymmetry of Mg–Nd alloys, a series of Mg–Nd alloys were hot extruded. The microstructure, hardness, tensile and compressive properties of Mg–Nd binary alloys at room temperature were studied.

2 Experimental procedure

2.1 Alloy preparation

Pure Mg and binary Mg–xNd (x = 0.2, 0.5, 1, 2, 5) alloys were prepared by permanent mould direct chill casting, cast in MagIC (Magnesium Innovation Centre), Geesthacht, Germany. High-purity Mg (MEL, UK, 99.94 wt.%) and Pure Nd (Grirem, China, 99.5 wt.%) were melted in a steel crucible under a protective atmosphere (Ar +2% SF_6) at a melt temperature of 750 °C, and the melt was stirred at 200 rpm for 20 min. The melt was poured into a steel mould (1.0044, EU Grade) and cooled with water (~15°C). The cast ingots were cylinder with 120 mm in diameter and 220 mm in height.

Extrusion treatment was used to obtain fine grains, performed at Fachgebiet Metallische Werkstoffe in TU Berlin, Germany. The as-cast pure Mg and Mg–Nd binary alloys ingots were machined to 93 mm in diameter. The ingots were homogenized at 440 °C using an electromagnetic induction furnace and extruded to round bars with 12 mm in diameter by indirect extrusion method. The extrusion rate was set to 0.6 m/s.

2.2 Microstructure analysis

Specimens were taken from the same location in different cast ingots and extruded bars for microstructure analysis. The X-ray fluorescence (XRF) (Bruker Explorer S4) method was used to determination of the chemical compositions of all the alloys. A digital camera (Leica TYPE 020-520.008 DM/LM) and a scanning electron

microscope (SEM) equipped with an energy dispersive X-ray (EDS) (Zeiss Ultra 55) were used to observe the microstructure of the alloys. The gran sizes of alloys were determined by line intercept methods (ASTM standard E 112-13) [15]. The pure Mg and Mg–5Nd alloy were analyzed by X-ray diffraction (XRD) using a diffractometer (Siemens D5000) with Cu K-α_1 radiation (wavelength λ = 0.15406 nm). The measurements were carried out at 40 kV and 40 mA, with a step size of 0.02°.

2.3 Mechanical property test

Vickers hardness was performed on studied alloys to investigate the influence of Nd content on the hardness properties. Specimens were prepared by grinding up to 2500 grit with silicon carbide emery paper. A Vickers hardness testing machine (KARL FRANK GMBH) were used to obtain the hardness of alloys with a 5 kg load, a 10 second dwell time, and 10 measurements were made for each specimen.

The compressive and tensile properties of Mg–Nd alloys were tested at room temperature using a static materials testing machine (Zwick 050) according to DIN EN 10002[16] and DIN 50106[17], respectively. The compressive specimens were cylinders of height 16.5 mm and diameter 11 mm. The tensile specimens had a 6 mm diameter, 30 mm gauge length, and threaded heads. The strain rate was set up as 1×10^{-3} s^{-1} for all tests and at least 3 specimens were measured under each condition.

3 Results

Chemical composition of alloys is listed in Table Ⅰ. There is low content of Fe (<0.030 wt.%), Cu (<0.002 wt.%) and Ni (<0.006 wt.%) in the alloys.

Table Ⅰ Chemical composition of studied alloys

Alloys (wt.%)	Nd (wt.%) [at.%]	Mg
Mg–0.2Nd	0.35 [0.05]	Balance
Mg–0.5Nd	0.67 [0.10]	Balance
Mg–1Nd	1.26 [0.18]	Balance
Mg–2Nd	2.39 [0.35]	Balance
Mg–5Nd	4.20 [0.63]	Balance

3.1 Microstructure

The optical microstructure pictures of as-cast Mg–Nd alloys are shown in Fig. 1. Very large grains (over 2 mm) and columnar morphology were formed in the alloys with 0.05–0.35 at.% Nd content. The grain size decreased significantly to 300 μmin Mg–5Nd alloy and equiaxed grains can be observed.

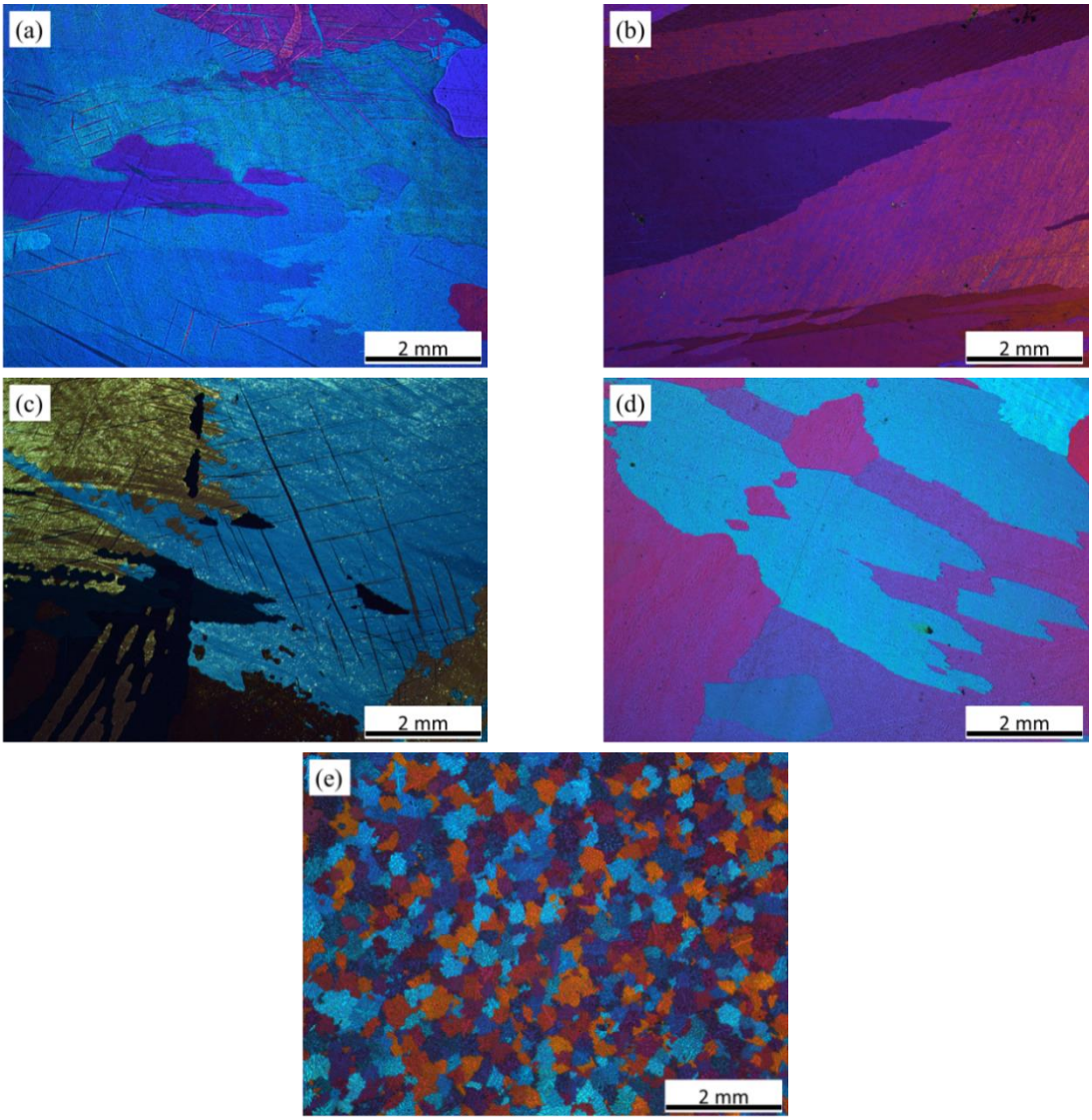

Fig. 1 Optical microstructures of as-cast Mg–Nd alloys: (a) Mg–0.2Nd; (b) Mg–0.5Nd; (c) Mg–1Nd; (d) Mg–2Nd; (e) Mg–5Nd.

Fig. 2 shows the optical microstructure of the samples which obtain from perpendicular to the extrusion direction. A large amount of the particles appears in the Mg–5Nd alloy (Fig. 2(e)).The optical microstructures which obtain along extrusion direction and the SEM images of extruded Mg–Nd alloys were reported in a previous study[18]. Fig. 2(f) shows the effect of Nd on alloy grain sizes. It is obvious that the grain size is inversely

proportional to the Nd content. Extrusion treatment refined grains of pure Mg to below 55 μm, the average grain size of Mg–Nd alloys decreased to 21 μm when the Nd content increased from 0.05 to 0.35 at.%. In particular, the grain size of Mg–5Nd was < 7 μm, which was caused by the large amount of intermetallic phase.

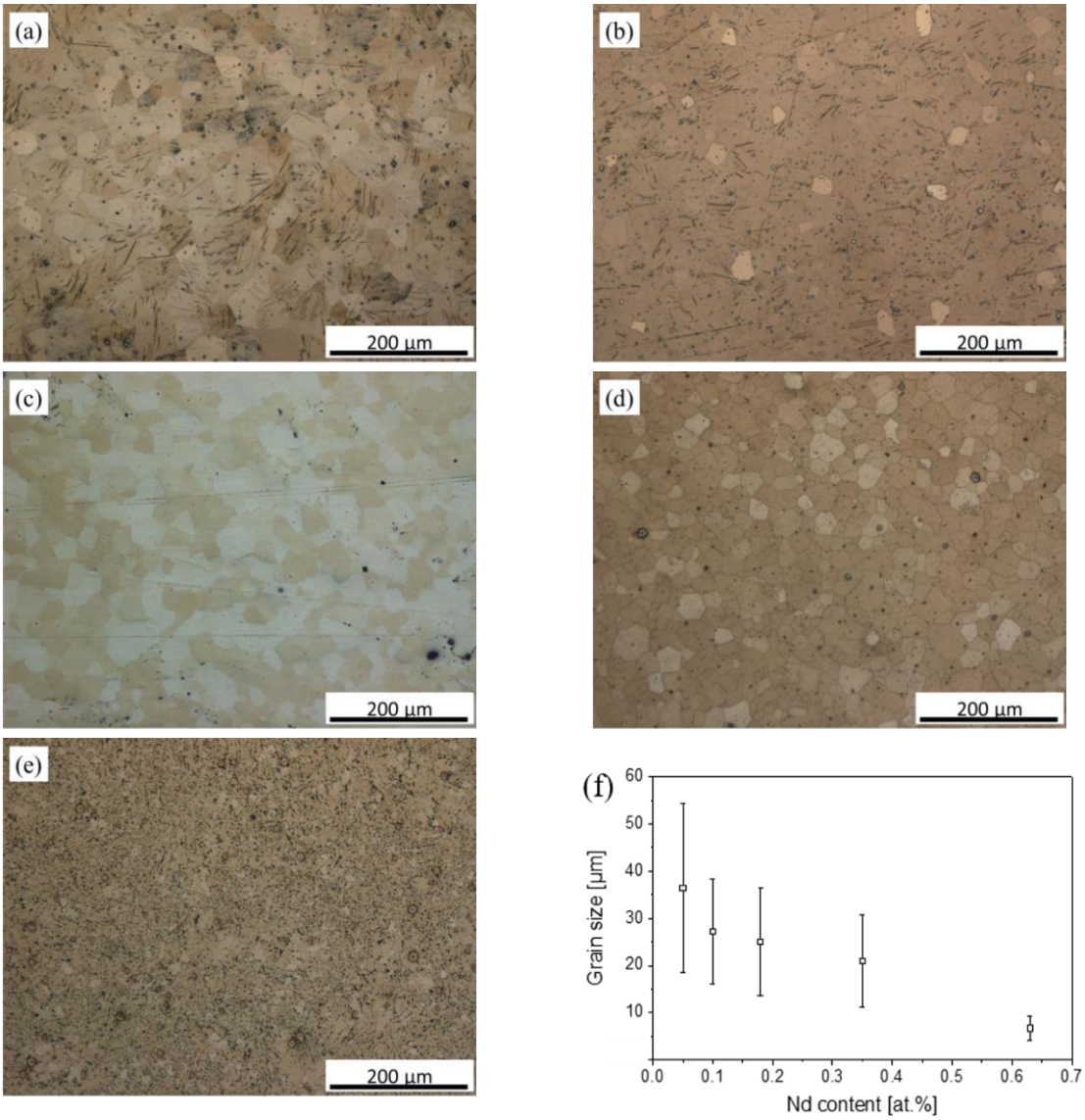

Fig. 2 Optical images of extruded Mg–Nd alloys obtained from the perpendicular to extrusion direction(a) Mg–0.2Nd;(b) Mg–0.5Nd; (c) Mg–1Nd; (d) Mg–2Nd; (e) Mg–5Nd;

(f) grain size of extruded Mg–Nd alloys.

The SEM analysis results of extruded Mg–5Nd alloy are shown in Fig. 3. A large number of white particles (1–2 μm) distribute on the Mg matrix, and EDX analysis was carried on the particles and matrix. A high Nd content (10.9 at.%) data was tested on the white particle (Position 1) and contained 89.1 at.% Mg. In the Mg matrix, like Position 2, there is little Nd (0.3 at.%) element.

Pure Mg and Mg–5Nd alloy after extrusion were selected for XRD phase analysis. The XRD test result shows that the $Mg_{41}Nd_5$ phase were formed in Mg–5Nd alloy (Fig. 3(b)). Additionally, the TEM micrograph of the second phase and the corresponding diffraction pattern was published in the previous study [18]. The diffraction pattern of the particles agreed with the data of the $Mg_{41}Nd_5$ phase, there were no micro-cracks at interface between Mg matrix and $Mg_{41}Nd_5$.

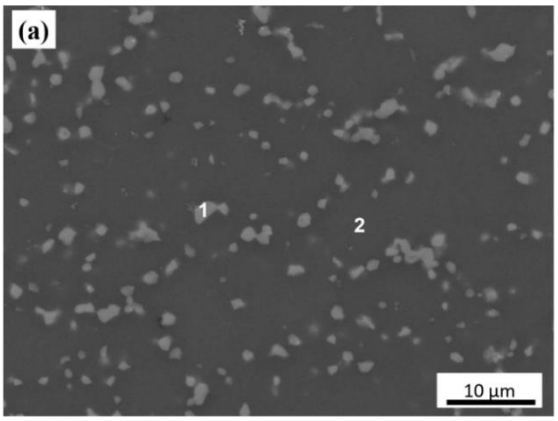

Position	Element	Conc. [wt.%]	Atomic [%]
1	Mg	62.4	89.1
	Nd	37.6	10.9
2	Mg	98.4	99.7
	Nd	1.6	0.3

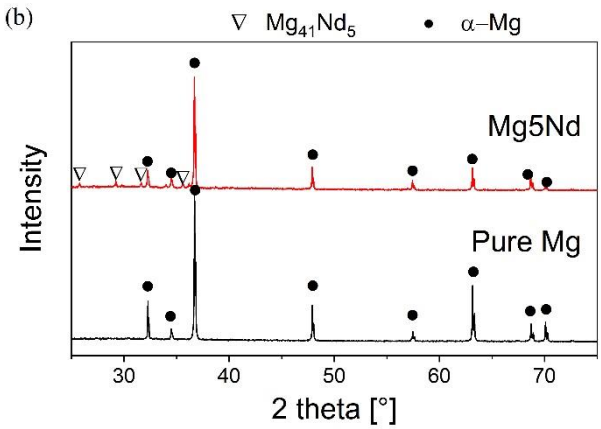

Fig. 3 (a) SEM images of Mg–5Nd alloy and EDS analysis result.

(b) XRD pattern of the extruded pure Mg and Mg–5Nd alloy.

3.2 Mechanical properties

Fig. 4 shows the tensile and compressive test results of extruded Mg–Nd alloys. After extrusion, the tensile yield strength (TYS) showed a small change with the 0–0.35 at.% Nd content which remain about 80 MPa; after Nd content approached 0.63 at.%, the TYS increased from 86 MPa to 133 MPa. Similarly, the ultimate tensile strength (UTS) of extruded alloys stabilized at around 190 MPa for 0–0.35 at.% Nd alloys; the UTS of Mg–5Nd

alloy was 224 MPa (Fig. 4(b)). The addition of Nd greatly improved the elongation of Mg alloys (Fig. 4(c)). The maximum elongation (33.5%) was obtained from extruded Mg–2Nd alloy.

An increase in Nd leads to increase in the compressive yield strength (CYS) for extruded alloys (Fig. 4(a)). For Mg–5Nd alloy, the CYS was much higher than other alloys. Maximum CYS were obtained from extruded Mg–5Nd at 146 MPa. The alloys with 0–0.18 at.% Nd had similar ultimate compressive strength (UCS) (Fig. 4(b)). After increasing Nd content to 0.35 at.%, the UCS increased from 310 MPa to 380 MPa. The compressibility was similar between the alloys at ~20% (Fig. 4(c)). Only the compressibility of Mg–0.5Nd alloy was 16%.

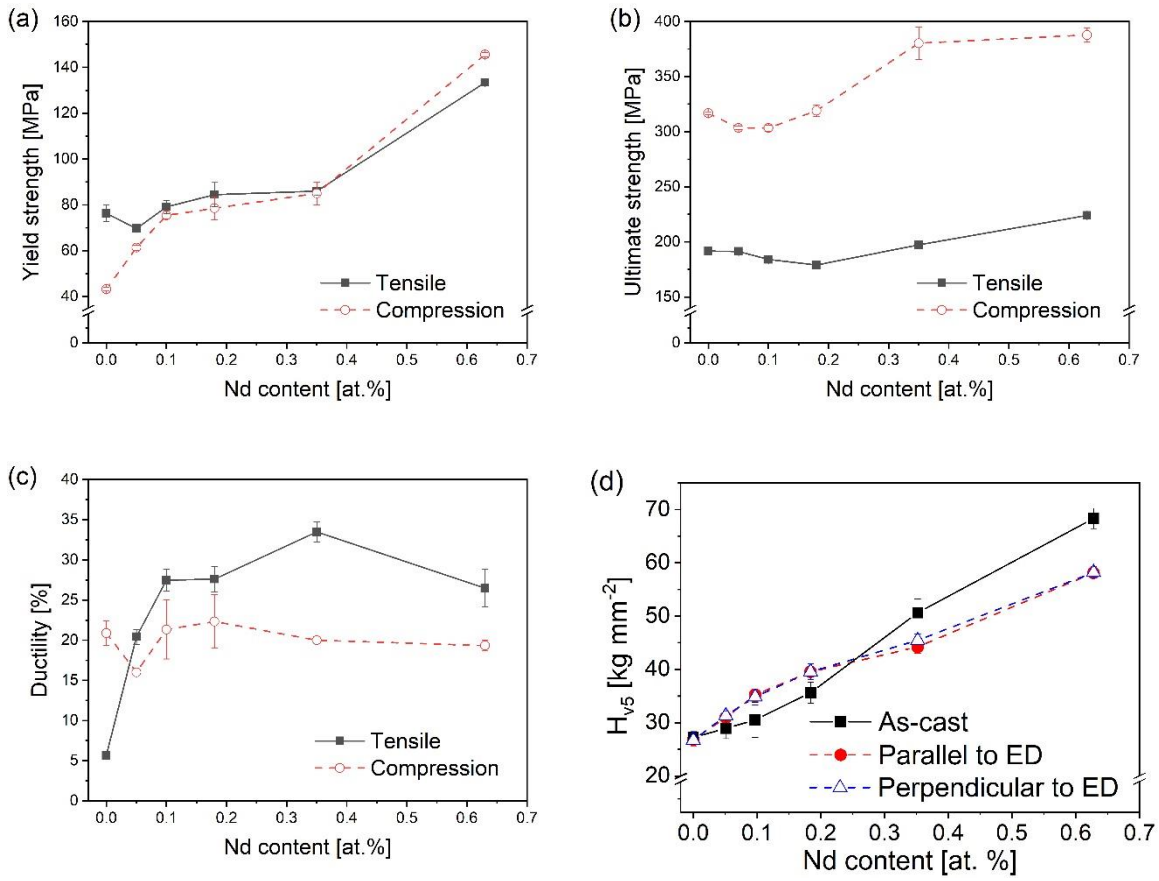

Fig. 4 Tensile and compression test result of extruded Mg–Nd alloys: (a) yield strength; (b) ultimate strength; (c) ductility, and (d) hardness of the Mg–Nd alloy. Error bars are standard deviations.

The Vickers hardness values of Mg–Nd alloys are shown in Fig. 4(d). For as-cast alloys, compared with pure Mg (27.2 kg mm^{-2}), the hardness increases with the increase in Nd content and reaches around 68 kg mm^{-2} for Mg–5Nd alloy. The Vickers hardness tests were applied on the parallel and perpendicular sides with respect to extrusion direction for Mg–Nd. The results show no difference in hardness from either side. The Vickers

hardness of pure Mg was around 25 MPa, and the Nd greatly improve the hardness of Mg alloys, the highest hardness was around 60 MPa for Mg–5Nd alloy. Compared with as-cast alloys, with low Nd content (0.05–0.18 at.%), the extruded alloys had a higher hardness value. However, with high Nd content (0.35 and 0.63 at.%), the alloys with lower hardness after extrusion.

4 Discussion

4.1 Strengthening mechanisms of Mg–Nd alloys

The microstructure study of the Mg–Nd alloys showed that the $Mg_{41}Nd_5$ particles are distributed in Mg matrix. Due to the limited solid solubility of Nd in Mg, strengthening caused by particles plays a very important role in this case. Contributions of strengthening mechanisms by the particles and atoms in solid solution have been analyzed using existing strengthening mechanism models.

4.1.1 Geometric characteristics

A previous study showed that the Nd in Mg–0.2Nd, Mg–0.5Nd and Mg–1Nd alloys was solid solute in Mg matrix[18]. The $Mg_{41}Nd_5$ appeared in Mg–2Nd and Mg–5Nd alloys. In this study, the following assumptions were made: 1) a perfect interface between the $Mg_{41}Nd_5$ particles and the matrix; 2) the particles have the same size; 3) their distance is identical; 4) they are homogeneously distributed; 5) the geometrical shape of particles is sphere.

The geometric characteristics of microstructure of Mg–2Nd and Mg–5Nd alloys are listed in Table Ⅱ, where d is the grain size, d_p is the mean diameter of the $Mg_{41}Nd_5$ particles, λ is the mean center-to-center spacing between particles, f_p is the volume fraction of $Mg_{41}Nd_5$ particles, mean spacing between the mean of partials is given by [19]

$$\lambda = \frac{1}{2} d_p \sqrt{\frac{3\pi}{2f_p}} \tag{1}$$

The d_p and λ were determined by SEM images.

Table Ⅱ Geometric characteristics of microstructure of the Mg–Nd alloys.

Materials	d [μm]	d_p [μm]	λ [μm]	f_p [%]
Mg–2Nd	21.0	1.5	12.5	1.7
Mg–5Nd	6.7	2.0	8.1	7.2

4.1.2 Strengthening mechanisms

The size, distribution and content of particles have effects on the strength of polycrystalline Mg alloy with discrete intermetallic phase, and the nature of the interface between the phases and the matrix also influence on the mechanical properties. In this study, the $Mg_{41}Nd_5$ phase has different crystal structure with Mg matrix, which means that the interface between the $Mg_{41}Nd_5$ phase and Mg matrix is to be incoherent state. The strengthening mechanisms of Mg–2Nd and Mg–5Nd alloys are divided into the following:

1) dislocation looping with particles(Orowan process), $\Delta\sigma_{p_O}$;
2) load transfer between a matrix and a particle, $\Delta\sigma_{\mathrm{LT}}$;
3) strengthening by dislocation generation, $\Delta\sigma_{p_d}$;
4) grain boundary strengthening, $\Delta\sigma_{\mathrm{g}}$;
5) solid solution strengthening, σ_{s}.

An increase in yield stress due to the Orowan process $\Delta\sigma_{p_O}$ can be given by [20]

$$\Delta\sigma_{p_O} = \frac{0.81\,MGb}{2\pi(1-\nu)^{\frac{1}{2}}}\frac{\ln\left(\frac{d_{\mathrm{p}}}{b}\right)}{(\lambda - d_{\mathrm{p}})} \tag{2}$$

where M is the Taylor factor and is 2.5 for Mg polycrystals with texture [21], G is the shear modulus (= 1.66 × 10^4 MPa for Mg [22]) b is the Burgers vector (= 3.21 × 10^{-10} m for Mg), and ν is the Poisson's ratio.

The strengthening mechanism which caused by load transfer $\Delta\sigma_{LT}$ between a matrix and a particle could be quantitatively given by:

$$\Delta\sigma_{\mathrm{LT}} = (\sigma_{\mathrm{m}} + \sigma_{\mathrm{s}})\frac{1}{2}f_p \tag{3}$$

where σ_m, is the yield stress of a matrix [23]. In this study, the values of σ_m for the Mg–Nd alloys are taken to be 10.06 and 10.75 MPa for tensile and compression test, respectively, which are the yield stresses of pure Mg [24].

The inconsistency between the matrix and the second-phase particles can increase the rate of dislocation generation which result in an increased strain hardening rate. The expression for the required stress is as follows:

$$\Delta\sigma_{p_p} = \alpha Gb\left(\frac{f_{\mathrm{p}}8\gamma}{bd_{\mathrm{p}}}\right)^{\frac{1}{2}} \tag{4}$$

where γ is the shear strain [2].

Hall–Petch Equation is used to estimate the influence of the grain size on the yield stress [25, 26],

$$\Delta\sigma_{\mathrm{g}}=kd^{-1/2} \tag{5}$$

where d is the mean grain size, k is a constant (= 0.18 and 0.25 MPa $m^{1/2}$ for tensile and compression test, respectively) [25].

The Nd solid solute effect on yield stress was observed by following the equation for Mg–0.05~0.18 at.% Nd alloys

$$\sigma_{\mathrm{s}} = \sigma_{0.2} - (\sigma_{\mathrm{m}} + \Delta\sigma_{\mathrm{g}}) \tag{6}$$

In this case, the Nd maximal solid solubility in Mg was 0.18 at.%, which means the contribution from solid solution strengthening of Mg–2Nd and Mg–5Nd alloys were the same as Mg–1Nd alloy.

The individual contributions of strengthening mechanisms to the yield stress of Mg–2Nd and Mg–5Nd alloys are listed in Table Ⅲ for tensile and compression tests, respectively. The results show that the total values of both tensile and compressive yield stresses calculated by the strengthening mechanisms are highly agreement with experimental values for Mg–5Nd alloy. But the predicted values of the Mg–2Nd alloy were higher than experimental data. The content of $Mg_{41}Nd_5$ in Mg–2Nd alloy is quite low, which means an error existed in the calculation, and caused the different values for experiment and calculation.

Table Ⅲ Contribution of strengthening mechanisms to the TYS and CYS of Mg–Nd alloys.

Materials		Individual strengthening [MPa]							
		$\Delta\sigma_{\mathrm{LT(T)}}$	$\Delta\sigma_{p_d}$	$\Delta\sigma_{p_O}$	$\Delta\sigma_{\mathrm{g(T)}}$	$\sigma_{\mathrm{m(T)}}$	$\sigma_{\mathrm{s(T)}}$	σ_{total}	$\sigma_{0.2\%\mathrm{(T)}}$
TYS	Mg–0.2Nd	-	-	-	29.79	10.06	29.82	-	69.67
	Mg–0.5Nd	-	-	-	34.51	10.06	34.55	-	79.12
	Mg–1Nd	-	-	-	36.00	10.06	38.37	-	84.43
	Mg–2Nd	0.42	7.92	1.57	39.28	10.06	38.37	97.60	87.00
	Mg–5Nd	0.76	14.11	2.93	69.54	10.06	38.37	136.75	133.40
CYS	Mg–0.2Nd	-	-	-	41.38	10.75	8.87	-	61.00
	Mg–0.5Nd	-	-	-	47.94	10.75	16.75	-	75.43
	Mg–1Nd	-	-	-	50.00	10.75	17.75	-	78.50
	Mg–2Nd	0.11	7.92	1.57	54.55	10.75	17.75	92.78	85.00
	Mg–5Nd	0.48	14.11	2.93	96.58	10.75	17.75	143.14	145.53

4.2 Effect of Nd content on tension-compression yield asymmetry

Fig. 5(b) and (c) present the tensile and compressive stress-strain curves of pure Mg and Mg–5Nd alloy respectively. The Mg–5Nd alloy showed excellent ductility. Pure Mg and Mg–5Nd alloy show significant differences in anisotropy. For pure Mg, it is obvious that there is a very large difference in the tensile and compressive yield behavior; the yield strengths and the rate of work hardening are lower in compression than in tension. The yield strength rates of tension–compression asymmetry were calculated and are presented in Fig. 5(c). The increasing amount of Nd content improved the asymmetry behavior. The TYS/CYS ratio of extruded Mg–Nd alloys decreased from 1.77 to 0.91 when Nd content increased from 0 to 0.63 at.%; the Mg–2Nd alloy the asymmetry ratio reached 1.01. Little asymmetry in the yield behavior can be observed from Mg–Nd alloys.

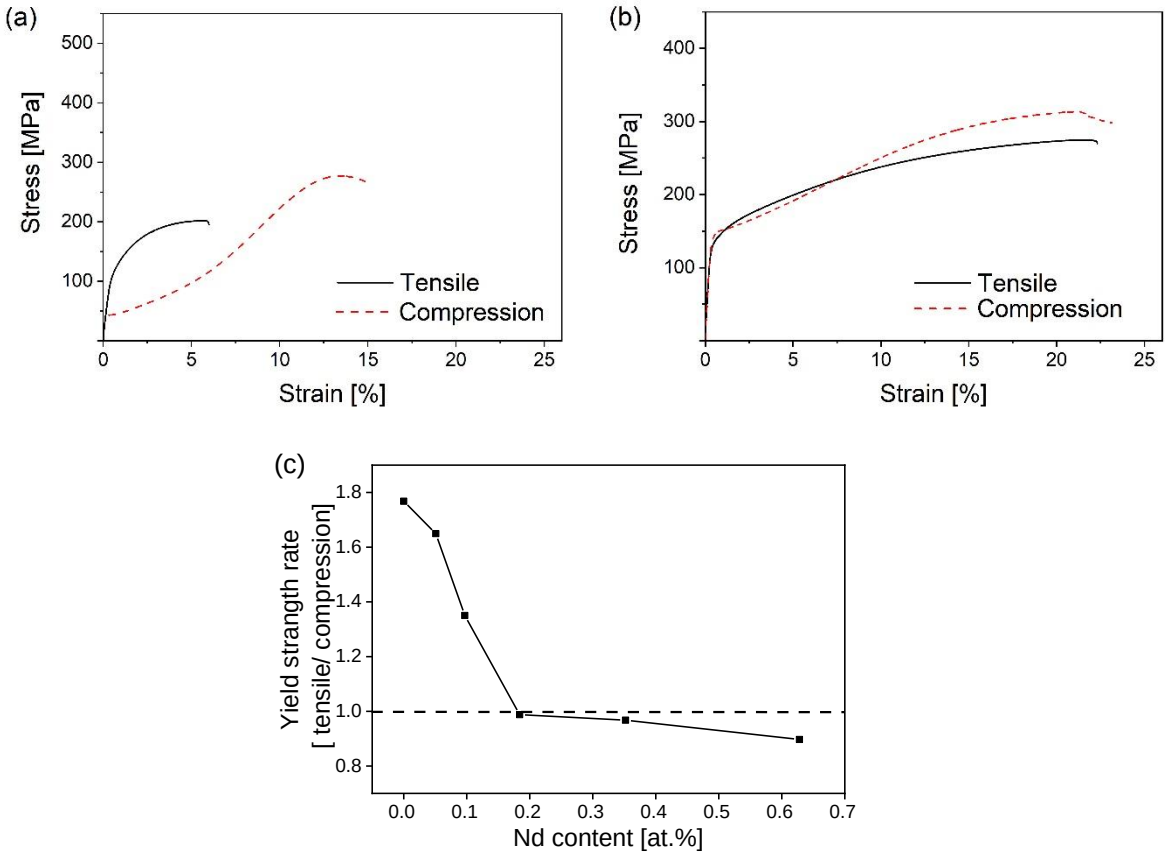

Fig. 5 True stress-strain curves of extruded (a) pure Mg and (b) Mg–5Nd alloy;

(c) tension-compression asymmetry in yield behavior of extruded Mg–Nd alloys.

Second phase particles can have a significant effect on the recrystallization behavior, texture, and mechanical properties, due to its effects on the microstructure. In addition to the particle deformation zone (PDZ) also possibly being formed at the particle area during extrusion, the deformation zones for large particles (d >1μm)

can be the source of particle stimulated nucleation (PSN) of recrystallization [28, 29].This means that a large number of potential nuclei with a large spread of orientations are formed and ready to contribute to PSN during recrystallization. The explanation for the lack of asymmetry in tensile-compressive yield behavior and random texture observed in Mg–Nd alloys, is that recrystallization has occurred mainly by PSN [30]. On the other hand, the Nd in solid solutes can lead to changes in deformation mechanisms which change the slip and twin system activity during extrusion. Moreover, those solid solutes can lead to the different texture and weaken the texture of Mg alloys which is most likely due to the occurrence of dynamic strain aging (DSA) [31, 32]. The texture behaviors will require separate investigation in the future.

5 Conclusion

The contributions of different strengthening mechanisms of extruded Mg–Nd alloys were investigated. Contributions of solid solution strengthening in Mg–xNd alloys (x = 0.2, 0.5, 1, 2, 5) were calculated. These contributions reached 38.37 and 17.75 MPa for tensile and compression yield stress, respectively, when Nd content increased to the maximal solid solubility (0.18 at.%). The highest Nd content alloy showed both highest yield strength and ultimate strength. The high strength was attributed to the grain boundary strengthening mechanisms. A large amount of $Mg_{41}Nd_5$ phase reduced the grain size from 21 to 7 μm. Thus, the contribution to yield stress of Mg–5Nd alloy from $Mg_{41}Nd_5$ phase strengthening and fine grain strengthening were 18 and 70 MPa, respectively, which were 10 and 30 MPa higher than those of Mg–2Nd alloy.

The tension-compression yield asymmetry at room temperature was investigated on extruded pure Mg and Mg–Nd binary alloys. Large tension-compression yield asymmetry ratio (1.77) can be observed in pure Mg, due to basal plane being preferentially parallel to the extrusion direction. Large amounts of second phase with size in 1–2 μm were observed in Mg–Nd alloys. The result shows little asymmetry in tension and compressive deformation behavior.

Acknowledgement

The authors would like to acknowledge the help of Mr. Günther Meister (HZG) during casting. The China Scholarship Council co-supported present work (Grant No. 201406890032).

References

1. K.U. Kainer, *Magnesium Alloys and Their Applications*, 1st ed. (Weinheim, Germany, Willey-VCH Verlag GmbH, 2003), pp. 1-20.
2. H.E. Friedrich, B.L. Mordike, *Magnesium Technology: Metallurgy, Design Data, Applications*, (Springer, Berlin, Germany, 2006), pp. 499-506.
3. T.B. Abbott, *Corros*., 71, 120 (2014).
4. N. Hort, Y. Huang, D. Fechner, M. Stormer, C. Blawert, F. Witte, C. Vogt, H. Drucker, R. Willumeit, K.U. Kainer, F. Feyerabend, *Acta Biomater*., 6,1714 (2010).
5. B. Smola, I. Stulıková, F. Von Buch, B. Mordike, *Mater. Sci. Eng.: A*, 324, 113 (2002).
6. L.L. Rokhlin, Magnesium Alloys Containing Rare Earth Metals: Structure and Properties, (CRC Press, London, UK, 2003).
7. N. Stanford, *Mater. Sci. Eng.: A*, 527, 2669 (2010).
8. P. Bakke, H. Westengen, The role of rare earth elements in structure and property control of magnesium die casting alloys, *Essential Readings in Magnesium Technology*, ed. S. Mathaudhu, A. Luo, N. Neelameggham, E. Nyberg and W. Sillekens (Switzerland, Springer, 2016), p. 313.
9. J.A. Yasi, L.G. Hector Jr, D.R. Trinkle, *Acta Mater*., 58, 5704 (2010).
10. G. Barucca, R. Ferragut, F. Fiori, D. Lussana, P. Mengucci, F. Moia, G. Riontino, *Acta Mater.*, 59, 4151 (2011).
11. J.F. Nie, *Scr. Mater*., 48, 1009 (2003).
12. Y.M. Savitskii, V.Terekhova, I. Novikova, *Zh. Neorg. Khim.*, 3, 2138 (1958).
13. J. Yan, Y. Sun, F. Xue, S. Xue, W. Tao,*Mater. Sci. Eng.: A*, 476, 366 (2008).
14. Z. Tian, Q. Yang, K. Guan, J. Meng, Z. Cao, *J. Alloys Compd*., 731, 704 (2018).
15. ASTM International (2013), Standard Test Methods for Determining Average Grain Size (ASTM E112-13).
16. DIN (2017), Metallic Materials - Tensile Testing - Part 1: Method of Testing at Ambient Temperature (DIN EN ISO 6892-1).
17. DIN (2016), Testing of metallic materials- Compression test at room temperature (DIN 50106:2016-11).
18. Y. Xu, L. Wang, M. Huang, F. Gensch, K.U. Kainer, N. Hort, *Adv. Eng.Mater*., (2018).
19. G. Le Roy, J. Embury, G. Edwards, M. Ashby, *Acta Metal*., 29, 1509 (1981).
20. R. Aikin Jr, L. Christodoulou, *Scr. Metall. Mater.*, 25, 9(1991).

21. C. Cáceres, P. Lukáč, *Philos. Mag*., 88, 977 (2008).

22. H.J. Frost, M.F. Ashby, *Deformation Mechanism Maps: the Plasticity and Creep of Metals and Ceramics*, (Pergamon Press, Oxford, UK, 1982), 43-44.

23. A.E. Ares, C.E. Schvezov,*J. Metall.*, 1,(2013).

24. Y. Xu, F. Gensch, Z. Ren, K.U. Kainer, N. Hort, *Prog. Nat. Sci.: Mater. Int.*, 28, 724 (2018).

25. E. Hall, *Proc. Phys. Soc., London, Sect. B*, 64,747 (1951).

26. N.J. Petch, *J. Iron Steel Inst.*, 174, 25 (1953).

27. D. Nagarajan, C.H. Cáceres, J.R. Griffiths, *Metal. Mater. Trans. A*, 45, 5401 (2016).

28. E. Ball, P. Prangnell, *Scr. Metall. Mater.*, 31, 2 (1994).

29. X. Xu, X. Chen, W. Du, Y. Geng, F. Pan, *J. Mater. Sci. Technol.*, 33, 9 (2017).

30. L. Mackenzie, B. Davis, F. Humphreys, G. Lorimer, *Mater. Sci. Technol.*, 23, 1173 (2007).

31. J. Bohlen, S. Yi, D. Letzig, K.U. Kainer, *Metal. Mater. Trans. A*, 527, 7092 (2010).

32. K. Hantzsche, J. Bohlen, J. Wendt, K.U. Kainer, S.B. Yi, D. Letzig, *Scr. Mater.*, 63, 725, (2010).